

The influences of $\text{LaVO}_4:\text{Eu}^{3+},\text{Cr}^{3+}$ red phosphors on white light-emitting diode applications

Nguyen Hung Khanh¹, Nguyen Le Thai², Thuc Minh Bui³, Huu Phuc Dang⁴, Huynh Thanh Thien⁵

¹Faculty of Engineering, Dong Nai Technology University, Bien Hoa City, Vietnam

²Faculty of Engineering and Technology, Nguyen Tat Thanh University, Ho Chi Minh City, Vietnam

³Faculty of Electrical and Electronics Engineering, Nha Trang University, Nha Trang City, Vietnam

⁴Faculty of Fundamental Science, Industrial University of Ho Chi Minh City, Ho Chi Minh City, Vietnam

⁵Faculty of Electrical and Electronics Engineering, Ton Duc Thang University, Ho Chi Minh City, Vietnam

Article Info

Article history:

Received Oct 28, 2023

Revised Nov 30, 2023

Accepted Dec 6, 2023

Keywords:

Color rendering

Color uniformity

$\text{LaVO}_4:\text{Eu}^{3+},\text{Cr}^{3+}$

Lumen output

Red phosphors

ABSTRACT

In this present paper, the $\text{LaVO}_4:\text{Eu}^{3+},\text{Cr}^{3+}$ (LV:Eu,Cr) red-orange phosphors are introduced in WLED fabrication. The LV:Eu,Cr phosphor is synthesized with high-temperature solid-phase reaction. The luminescence properties of the phosphor are monitored with ultraviolet-visible and near-infrared (UV-vis-NIR) measurements. The heat generating in the phosphor sample is also investigated with different power densities of the 980 nm laser. The phosphor exhibits absorption bands at 254 nm and 316 nm, suitable for UV light-emitting diodes (UV LED) applications. The Cr^{3+} concentrations have noticeable effects on the luminescence of the phosphor. The increasing Cr^{3+} dosage initiates reduction in Eu^{3+} emission intensity and luminescence lifetime average. The heat-activated amount in the phosphor is also significant with the higher concentration of Cr^{3+} ions. When using the LV:Eu,Cr phosphor in white light-emitting model (WLED), the dominant red-orange emission centered at 595 nm is observed, in addition to the blue peak at 453 nm. The luminosity, color rendition, and color uniformity of the WLED light are also discussed. The findings indicate that the phosphor can be combined with other high-efficiency blue and green phosphors to obtain the improved color rendition and luminous performances and used in heat-creating optical applications.

This is an open access article under the [CC BY-SA](https://creativecommons.org/licenses/by-sa/4.0/) license.



Corresponding Author:

Huynh Thanh Thien

Faculty of Electrical and Electronics Engineering, Ton Duc Thang University

Ho Chi Minh City, Vietnam

Email: huynhthanhthien@tdtu.edu.vn

1. INTRODUCTION

Rare earth-doped phosphors have a variety of uses in modern technology, including in the production of magnets, lasers, optical fibers, and medical applications such as in imaging and cancer treatment [1], [2]. Moreover, such luminescent materials are commonly utilized in various lighting applications, including fluorescent lamps, light-emitting diodes (LEDs), and cathode-ray tubes. Particularly, these rare-earth-doped phosphors offers sharp and strong emission when excited in the ultraviolet-visible (UV-Vis) and near-infrared (NIR) wavelengths [3], [4]. For example, in the NIR area, the Nd:YAG laser gives intense and broad emission band, sufficient for various applications [5]. Besides, they are used to fabricate biosensors by combining with biomolecules [6]. Additionally, when using in white LED production, as excited by an external energy source, such as a UV or blue light, these materials absorb energy and then release it as visible light. The color of the emitted light depends on the specific rare earth ion used and the

properties of the host matrix. Furthermore, it is possible to enhance the luminescence strength of rare-earth dopants in host substances by integrating other rare-earth classes to act as sensitizers [7]–[9]. One of the most investigated rare-earth dopants is the trivalent europium Eu^{3+} . This rare-earth ion gives the bright red emission suitable for display applications and strong far-infrared lasing emission. It is also doped in various host materials including glass matrix, micro phosphors, nanophosphors, and bio-mediums. Owing to its multiple energy levels, it can yield sharp 610 nm–615 nm red band when being doped in most of these host lattices. Besides, the bright red emission, their emission includes the orange (590 nm) and deep red regions (~650 nm and 700 nm). Moreover, previous studies reported that Eu^{3+} -doped luminescent material could give stronger emission in red regions and greater luminescent performance than many other phosphor materials, owing to its narrow-band emission and long optical-active lifetime [10]–[12]. With such emission properties, Eu^{3+} -doped phosphors are often utilized in LEDs in combination with blue- and green-emission materials for achieving high-color-rendition white light. In most of the host materials, however, the Eu^{3+} is often self-activated, and the emission in orange and deep red in neutral red (NR) region are relatively weak [13], [14].

In this study, we use the LaVO_4 (LV) phosphor as the host material for doping the Eu^{3+} ions. The LV phosphor is self-activated and has high UV-light absorption efficiency. It also gives blue emission of 350–450 nm that can be well-absorbed by the Eu^{3+} ion dopants. After taking in such lights, the Eu^{3+} ion emits them in the region from 240 nm to 750 nm. Then, for the sensitizer, the Cr^{3+} ion is chosen as it can give wide emission range from blue to red, long lifetime phosphorescence due to its long-lived $2E$ state, and laser emission in either NIR or infrared areas. Besides, when being in the same host matrix, the Eu^{3+} is likely to transfer its energy by a small amount to the Cr^{3+} , as the $4T_1(4F)$ energy level of the Cr^{3+} ion stays below the energy level $5D_0$ of Eu^{3+} [15]–[17]. This can initiate the decrease of Eu^{3+} luminescence-intensity lifespan. The phosphor $\text{Eu}^{3+}, \text{Cr}^{3+}$ -doped LV ($\text{LV}:\text{Eu}, \text{Cr}$) phosphor is synthesized via the solid-phase reaction at high temperatures. Then, its luminescence and heat production are investigated. The phosphor is also used to build the conventional WLED model with blue LED and $\text{YAG}:\text{Ce}^{3+}$ phosphor. The $\text{LV}:\text{Eu}, \text{Cr}$ added dosage is varied for monitoring its influences on the light performances of the as-prepared white LED (WLED). The findings indicating the phosphor could be used for heat-generate application and solid-state LED lighting devices [18], [19].

2. METHOD

The synthesizing method for the $\text{LV}:\text{Eu}, \text{Cr}$ luminescent phosphor is the high-temperature solid-phase reaction with the fixed Eu^{3+} doping concentration of 1.0 mol%. The initial ingredients of the phosphor composition are listed in Table 1. The stages of phosphor producing process can be described as follows. All the components are evenly weighed and blended with acetone in an agate mortar. Next, the mixture undergoes a calcinating process in a furnace at ~1200°C for 5 hours after being transferred into alumina crucibles. When the calcinating time is over, the product is cooled down to room temperature and followed by grinding into fine powders [20]. The WLED model built with $\text{LV}:\text{Eu}, \text{Cr}$ phosphor, blue LED chips, and $\text{YAG}:\text{Ce}$ phosphor is shown in Figure 1. The phosphor film for placing above the LED chip has a thickness of 0.08 mm. The LED chip has the radiant flux determined at 1.16 W and the blue-emission peaks at 453 nm. Figure 1(a) displays the as-prepared WLED in reality. Figure 1(b) demonstrates the wire-bonded LED-chip cluster. Figure 1(c) is the illustration for the cross-section of the WLED package, in which the arrangement of components is clearly depicted. Figure 1(d) presents the 3D model of WLED simulation obtained with LightTools software.

The X-ray diffraction data of the $\text{LV}:\text{Eu}, \text{Cr}$ phosphor is obtained using an X-ray diffractometer from Rigaku, Japan (MiniFlex 600) and refined with Rietveld refinement by FullProf Suite. The morphology and the energy dispersive X-ray spectroscopy of the phosphor are investigated with a scanning electron microscope unit (Zeiss EVO 18 research). Absorption spectral data of the phosphor is collected in the wavelength region from 200 nm to 800 nm with an UV-vis-NIR spectrophotometer (Lambda-750 PerkinElmer). The emission and excitation spectra of $\text{LV}:\text{Eu}, \text{Cr}$ phosphors are measured with the Horiba Fluorolog-3 coupled with a 450-W xenon lamp and photomultiplier tube. The heat generation of the phosphor is examined with a thermo-couple setup excited with various power densities of a lasing diode of 980 nm for 5 minutes [21], [22].

Table 1. The ingredients of $\text{LV}:\text{Eu}, \text{Cr}$ composition

Ingredients	Purity (%)	Origin
La_2O_3	>99%	Himedia
V_2O_5	>99%	Alpha Aesar
Eu_2O_3	>99%	Merck
Cr_2O_3	>99%	Alpha Aesar

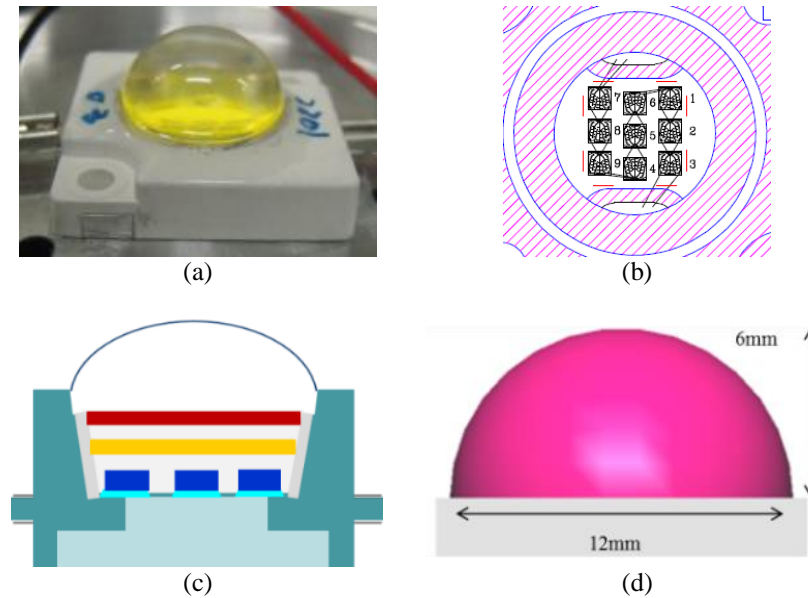


Figure 1. WLED structural demonstration: (a) a real WLED, (b) wire-bonded LED chips, (c) WLED cross-section, and (d) WLED simulation by LightTools

3. RESULTS AND DISCUSSION

3.1. Computational analysis of the phosphor luminescence

The phosphor samples of LV:Eu,Cr gives different bands of absorption owing to the discrepancies in the Eu³⁺ and Cr³⁺ charge distribution. The phosphor’s absorption spectra, recorded in the range from 200 nm to 400 nm, exhibits two significantly intense bands centered at wavelengths of 254 nm and 316 nm. When the doping dosage of the ion Cr³⁺ varies, the absorption intensities change while the position of absorption centers stay the same. To determine the optical energy gap (E_{gp}) of the phosphor with the absorption spectra, the Kubelka–Munk function ($F(R)$) and Tauc equation are utilized, as expressed in (1) and (2), respectively [23].

$$F(R) = (1 - R_{\infty})^2 / (2R_{\infty}) \tag{1}$$

$$F(R) = C \times (h\nu - E_{gp})^a / (h\nu) \tag{2}$$

where R_{∞} indicates the diffuse reflectance, $h\nu$ represents the incident-photon energy, and C is the band tailoring parameter. Here, a indicates the transition type, which is determined to be $1/2$ for the direct optical gap in this case. In the presence of increasing doping dosage of Cr³⁺ ions, there is a decline in the E_{gp} of the phosphor, owing to the material’s metallic nature.

The excitation spectra of the LV:Eu,Cr phosphor is examined with the emission wavelengths of 614 nm and 700 nm as the intense red emission is observed at these wavelengths for Eu³⁺ and Cr³⁺, respectively. The data show that the excitation spectra of the phosphor show the multiple peaks from 316 nm to 464 nm with the most eminent peak of 316 nm, in all cases. Besides, under the 700 nm emission, the excitation spectrum has an additional weak peak near 386 nm owing to the presence of Cr³⁺. As the Cr³⁺ concentration rises, the excitation peaks’ positions are unchanged but their intensity.

The emission spectra of the LV:Eu,Cr phosphor are examined under excitation wavelengths of 393 nm and 386 nm. The emission trend at 393 nm displays sharp bands within 420–750 nm regions, with the noticeable broad emission band in the deep red region (700–750 nm) assigned to the Cr³⁺ addition. The emission intensity of the phosphor shows reduction as the doping concentration of Cr³⁺ increases. This can be attributed to the energy transfer from the Eu³⁺ ions to Cr³⁺ ions. When being excited, the Eu³⁺ gives a small energy amount to the Cr³⁺, leading to the decrease in emission strength. This can be further determined with the luminescence lifetime of Eu³⁺ in the presence of Cr³⁺ in the phosphor host. Specifically, the lifetime of Eu³⁺ decreases with the increasing doping content of Cr³⁺. The decay curves of the luminescence under 393 nm excitation can be well fitted with the double exponential relation using (3):

$$I = A_1 e^{-t/\tau_1} - A_2 e^{-t/\tau_2} \quad (3)$$

where I represents the luminescent intensity at the time t ; τ_1 and τ_2 represent the lifetime of $\text{Eu}^{3+} \ ^5\text{D}_0$ levels [24]. Then, the luminescence lifetime average can be computed by (4).

$$I = \frac{A_1 \tau_1^2 + A_2 \tau_2^2}{A_1 \tau_1 + A_2 \tau_2} \quad (4)$$

In the thermal setup for the heat generation test, the LV:Eu,Cr phosphor produces great amount of heat when doping Cr^{3+} and this increases on the increase of Cr^{3+} content. The heat generation of the phosphor sample is also linked with the absorption of NIR radiation. Since both ions Cr^{3+} and Eu^{3+} absorb NIR light, they may potentially induce the heat creation in the phosphor. Additionally, the brown hue of the LV:Eu,Cr phosphors contributes generating heat in the samples owing to the thermal-phonon stimulation [25].

3.2. Phosphor influences on the WLED model's performance

The presence of LV:Eu,Cr phosphor has certain effects on the lighting properties of the WLED. Initially, the dosage of the YAG:Ce in the package should decrease to maintain the correlated color temperature (CCT) and induce the scattering activity. This can be seen in Figure 2, in which the increasing concentration of LV:Eu,Cr phosphor is followed by the gradual decrease of YAG:Ce amount. The scattering productivity of the phosphor package in the WLED is subsequently demonstrated in Figure 3. The data show that with the heightened doping amount of the LV:Eu,Cr phosphors, the scattering coefficient parameter increases, regardless of the light wavelengths. Such an improvement in light scattering can help stimulate the conversion efficiency for more red-emission color in and higher color uniformity.

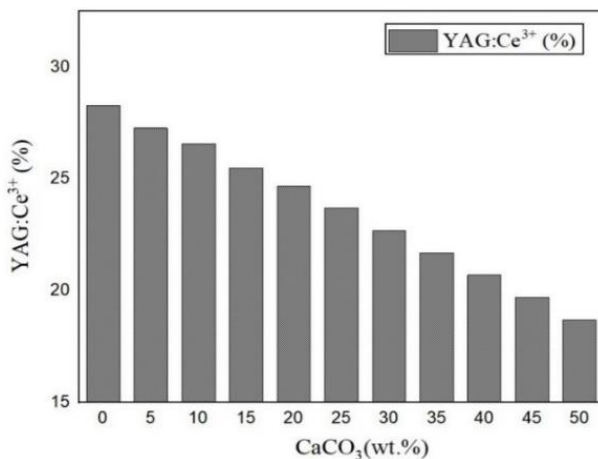


Figure 2. The concentration of YAG:Ce phosphor in the presence of increasing LV:Eu,Cr amount

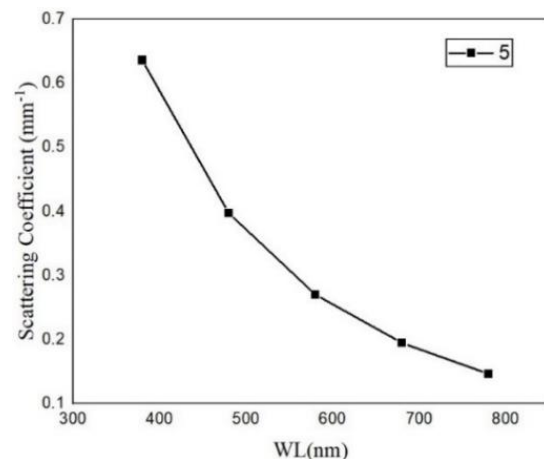


Figure 3. The scattering coefficients of the WLED phosphor package in the presence of LV:Eu,Cr phosphor

The angular CCT values and CCT variation tendency of the phosphor are presented in Figures 4 and 5, respectively. The angular CCT values of the WLED show significant variations as the concentration of the LV:Eu,Cr increases. The CCT line at 5 wt% LV:Eu,Cr nearly coincides with that at 0 wt% phosphor, indicating the influence of LV:Eu,Cr is not significant. On the increasing concentration of the LV:Eu,Cr phosphor, the CCT lines tend to decrease but with a very small amount. However, the CCT variation between different angles is large, which can be furthered discussed in Figure 5. As the CCT lines of 0-5 wt% of LV:Eu,Cr is nearly coincided, the CCT difference is not obvious. Continuously increasing the LV:Eu,Cr phosphor concentration leads to notably variations. The highest CCT difference is observed with 20 wt% while the lowest value is obtained at 40 wt% LV:Eu,Cr. So, it can achieve the highest color uniformity for the WLED with LV:Eu,Cr at 40 wt%.

The color fidelity of the WLED light can be further examined using the parameters of color rendering index (CRI) and color quality scale (CQS). Figures 6 and 7 depict the influence of increasing LV:Eu,Cr phosphor dosage on the CRI and CQS of the WLED, respectively. Particularly, both figures

display the reduction on the increase LV:Eu,Cr phosphor concentration. The decrease in CRI values is not as noticeable as that in the CQS case. The CQS includes all three imperative factors of CRI, observers' inclination, and coordination of colors. Therefore, it is influenced by many factors than the CRI. The lower CRI and CQS values in the presence of heightened LV:Eu,Cr concentrations imply the imbalance in color proportions on the chroma scale. This can be attribute to the increasing scattering events, creating the change in the proportion of elemental emission colors in the white light band. In this case, the red color tends to be induced owing to the absorption and conversion feature of the used phosphor. The phosphor LV:Eu,Cr presence induced the amount of visible light in the orange-red region (590-600 nm), see Figure 8. Though the blue emission intensity peak is presented, the peak at 595 nm is dominant. This also indicates the dominance of red emission on the chroma scale. Thus, the insufficient green and blue emission colors can result in the false reproduced color of the object with the incident light. With the ability to induce the eminent orange-red emission band, the LV:Eu,Cr phosphor can be used with other green-emitting and blue-emitting phosphors to increase the rendering factor of the WLED light [26]. The luminosity of the WLED light is the last factor investigated in this study. Figure 9 illustrates the obtained data about WLED lumen output with the increasing LV:Eu,Cr doping content. With 5 wt% LV:Eu,Cr dopant in the packages, the lumen intensity shows an increase but not noticeable. With higher concentration of LV:Eu,Cr in use, the luminous flux values gradually decrease, which can be assigned to the excessive scattering and absorption of light in the package, leading to the loss in total energy output. So, to get the decent lumen output, low content of LV:Eu,Cr, for example 5 wt%, should be chosen.

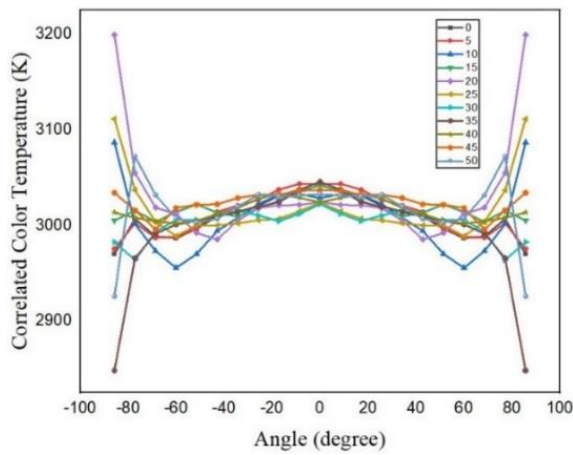


Figure 4. The angular CCT values of the WLED phosphor package in the presence of LV:Eu,Cr phosphor

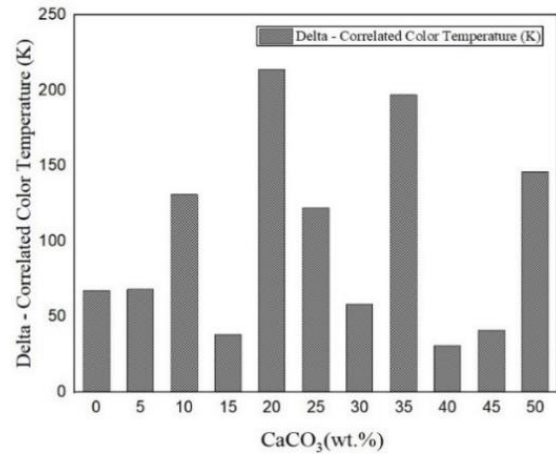


Figure 5. The CCT variations of the WLED phosphor package in the presence of LV:Eu,Cr phosphor

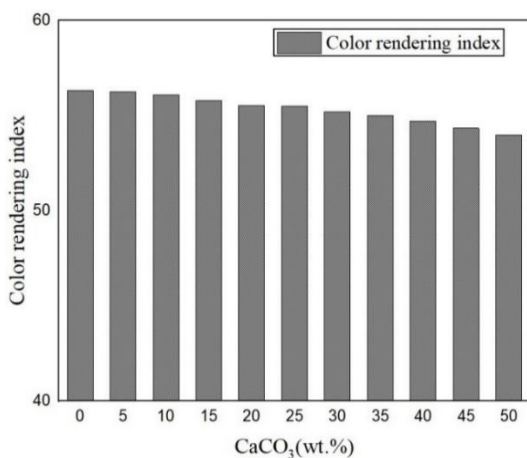


Figure 6. The CRI of the WLED phosphor package in the presence of LV:Eu,Cr phosphor

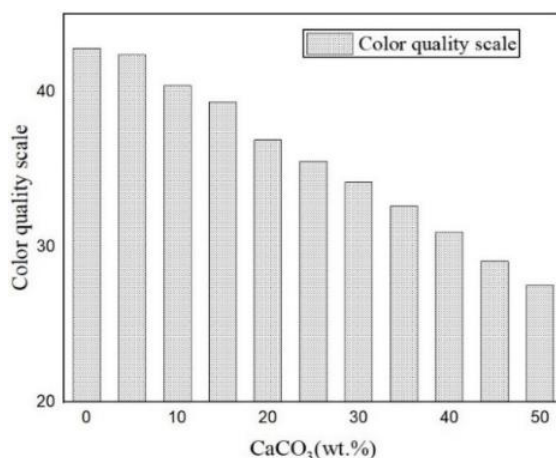


Figure 7. The CQS of the WLED phosphor package in the presence of LV:Eu,Cr phosphor

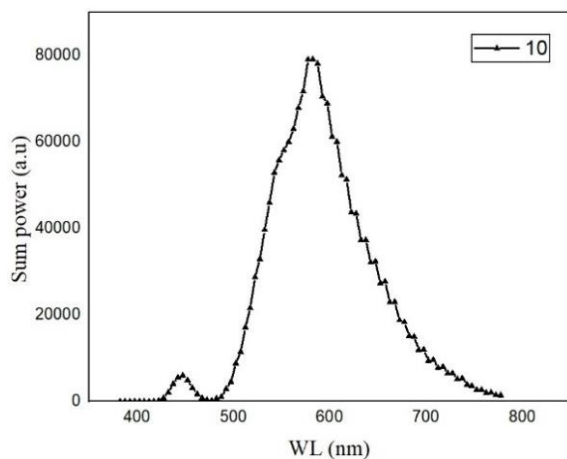


Figure 8. The sum power of the WLED phosphor package in the presence of LV:Eu,Cr phosphor

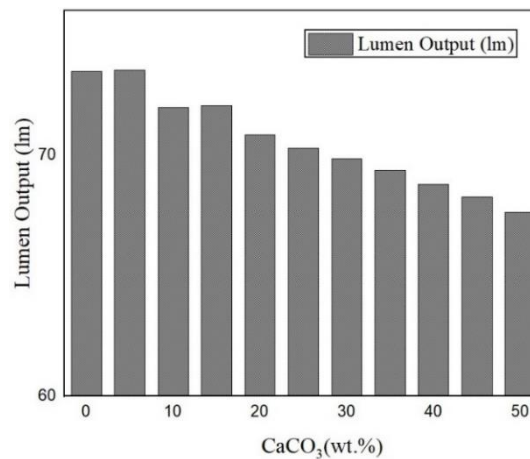


Figure 9. The lumen output of the WLED phosphor package in the presence of LV:Eu,Cr phosphor

4. CONCLUSION

The present study demonstrates the LV:Eu,Cr phosphor synthesized with high-temperature solid-phase reaction method. The phosphor shows absorption bands at 254 nm and 316 nm, suitable for UV LED applications. With the increasing dosage of Cr³⁺, the phosphor emission intensity decreases slightly owing to the energy transfer from the Eu³⁺ to Cr³⁺ ions. The addition of Cr³⁺ also induces the emission band in deep red region of around 700–750 nm. Moreover, the increase of Cr³⁺ stimulate the heat generation in the phosphor materials, suggesting that the phosphor can be used in heat-creating optical devices. In applying to fabricate the WLED package, the presence of LV:Eu,Cr give the eminent orange-red emission band with the peak at 595 nm. The weaker emission peak at 453 nm is also noticed, indicating that the phosphor can be excited by the blue LED chips. With the increasing LV:Eu,Cr concentration, the scattering efficiency is improved, and the lowest CCT deviation is obtained at 40 wt%. However, the CRI and CQS slightly decrease due to the imbalance in color proportions. The lumen output shows small increase with 5 wt% of LV:Eu,Cr but gradual decrease as the concentration of the phosphor further increases. Thus, the phosphor can be used in combination with other high-efficiency blue and green phosphor to obtain the higher color rendition and luminous performances.




REFERENCES

- [1] Y. Motonaga, T. Matsumoto, and N. Motonaga, "Color chart of European pear 'Le Lectier' based on the color image analysis," in *Proceedings of the SICE Annual Conference*, 2010, pp. 2455–2461.
- [2] X. Zhang, "A novel quality metric for image fusion based on color and structural similarity," in *2009 International Conference on Signal Processing Systems, ICSPS 2009*, 2009, pp. 258–262, doi: 10.1109/ICSPS.2009.72.
- [3] A. Kolaman and O. Yadid-Pecht, "Quaternion structural similarity: a new quality index for color images," *IEEE Transactions on Image Processing*, vol. 21, no. 4, pp. 1526–1536, Apr. 2012, doi: 10.1109/TIP.2011.2181522.
- [4] D. J. Lee, J. K. Archibald, and G. Xiong, "Rapid color grading for fruit quality evaluation using direct color mapping," *IEEE Transactions on Automation Science and Engineering*, vol. 8, no. 2, pp. 292–302, Apr. 2011, doi: 10.1109/TASE.2010.2087325.
- [5] R. Haruki and T. Hofuchi, "Improved and extended scalable image coding by spline approximation for a binary, gray-scale and color image," in *Proceedings - 7th International Conference on Parallel and Distributed Systems: Workshops*, 2000, pp. 31–38, doi: 10.1109/ICPADS.2000.857680.
- [6] C. Gao, K. Panetta, and S. Aghaian, "No reference color image quality measures," in *2013 IEEE International Conference on Cybernetics, CYBCONF 2013*, Jun. 2013, pp. 243–248, doi: 10.1109/CYBConf.2013.6617445.
- [7] Y. Yuan, Z. Guoqiang, C. Zhenwei, and G. Yudong, "Color image quality assessment with multi deep convolutional networks," in *2019 IEEE 4th International Conference on Signal and Image Processing, ICSIP 2019*, Jul. 2019, pp. 934–941, doi: 10.1109/SIPROCESS.2019.8868333.
- [8] K. Panetta, C. Gao, and S. Aghaian, "No reference color image contrast and quality measures," *IEEE Transactions on Consumer Electronics*, vol. 59, no. 3, pp. 643–651, Aug. 2013, doi: 10.1109/TCE.2013.6626251.
- [9] F. Zhang, J. Li, G. Chen, and J. Man, "Assessment of color video quality with singular value decomposition of complex matrix," in *5th International Conference on Information Assurance and Security, IAS 2009*, 2009, vol. 1, pp. 103–106, doi: 10.1109/IAS.2009.144.
- [10] K. Kotani, Q. Gan, M. Miyahara, and V. R. Algazi, "Objective picture quality scale for color image coding," in *IEEE International Conference on Image Processing*, 1995, vol. 3, pp. 133–136, doi: 10.1109/icip.1995.537598.
- [11] M. Omari, M. El Hassouni, H. Cherifi, and A. A. Abdelouahad, "On color image quality assessment using natural image statistics," in *Proceedings - 10th International Conference on Signal-Image Technology and Internet-Based Systems, SITIS 2014*, Nov. 2014, pp. 516–523, doi: 10.1109/SITIS.2014.60.




- [12] J. Yuan, J. Y. Hardeberg, and G. Chen, "Development and evaluation of a hybrid point-wise gamut mapping framework," in *2015 Colour and Visual Computing Symposium, CVCS 2015*, Aug. 2015, pp. 1–4, doi: 10.1109/CVCS.2015.7274889.
- [13] A. Samani, K. Panetta, and S. Aгаian, "Quality assessment of color images affected by transmission error, quantization noise, and noneccentricity pattern noise," in *2015 IEEE International Symposium on Technologies for Homeland Security, HST 2015*, Apr. 2015, pp. 1–6, doi: 10.1109/THS.2015.7225335.
- [14] A. R. Bagaskara, H. Prasetyo, and H. P. Alim Wicaksono, "Color-embedded-grayscale quality enhancement using deep convolutional networks," in *2020 27th International Conference on Telecommunications (ICT)*, Oct. 2020, pp. 1–5, doi: 10.1109/ict49546.2020.9239457.
- [15] D. Lee and K. N. Plataniotis, "Towards a full-reference quality assessment for color images using directional statistics," *IEEE Transactions on Image Processing*, vol. 24, no. 11, pp. 3950–3965, Nov. 2015, doi: 10.1109/TIP.2015.2456419.
- [16] M. H. Lee, H. Park, and J. Il Park, "Fast radiometric compensation accomplished by eliminating color mixing between projector and camera," *IEEE Transactions on Consumer Electronics*, vol. 54, no. 3, pp. 987–991, Aug. 2008, doi: 10.1109/TCE.2008.4637577.
- [17] S. Wang, J. Li, Q. Shen, B. Zhang, F. Zhang, and Z. Lu, "MODIS-based radiometric color extraction and classification of inland water with the fore-ule scale: A case study of lake Taihu," *IEEE Journal of Selected Topics in Applied Earth Observations and Remote Sensing*, vol. 8, no. 2, pp. 907–918, Feb. 2015, doi: 10.1109/JSTARS.2014.2360564.
- [18] K. Ma, T. Zhao, K. Zeng, and Z. Wang, "Objective quality assessment for color-to-gray image conversion," *IEEE Transactions on Image Processing*, vol. 24, no. 12, pp. 4673–4685, Dec. 2015, doi: 10.1109/TIP.2015.2460015.
- [19] B. Ahmad, H. Mutahira, M. Li, and M. S. Muhammad, "Measuring focus quality in color space," in *2019 2nd International Conference on Communication, Computing and Digital Systems, C-CODE 2019*, Mar. 2019, pp. 115–119, doi: 10.1109/C-CODE.2019.8681001.
- [20] J. Guo, P. Shrivastava, K. Kepley, S. Yang, S. Mitra, and B. Nutter, "Bit-rate allocation control and quality improvement for color channels in HMVQ image compression," in *Proceedings of the IEEE Symposium on Computer-Based Medical Systems*, 2004, vol. 17, pp. 110–115, doi: 10.1109/cbms.2004.1311700.
- [21] Y. Xiang, B. Zou, H. Wang, H. Li, and Z. Xie, "Multi-source color transfer for natural images," in *Proceedings - International Conference on Image Processing, ICIP*, 2008, pp. 469–472, doi: 10.1109/ICIP.2008.4711793.
- [22] Y. Chen, D. Li, and J. Q. Zhang, "Complementary Color wavelet: a novel tool for the color image/video analysis and processing," *IEEE Transactions on Circuits and Systems for Video Technology*, vol. 29, no. 1, pp. 12–27, Jan. 2019, doi: 10.1109/TCSVT.2017.2776239.
- [23] S. Qazi, K. Panetta, and S. Aгаian, "Detection and comparison of color edges via median based PCA," in *Conference Proceedings - IEEE International Conference on Systems, Man and Cybernetics*, Oct. 2008, pp. 702–706, doi: 10.1109/ICSMC.2008.4811360.
- [24] M. Xu, Y. Ma, and S. Chen, "Research on real-time quality inspection of PET bottle caps," in *2017 IEEE International Conference on Information and Automation, ICIA 2017*, Jul. 2017, pp. 1023–1026, doi: 10.1109/ICInfA.2017.8079052.
- [25] S. D. Thepade, P. Supriya, and A. Pawar, "Thorough performance analysis of haar, cosine, hartley and slant transforms for grayscale image colorization using thepade's transform error vector rotation algorithms in YCbCr and RGB color spaces," in *Global Conference on Communication Technologies, GCCT 2015*, Apr. 2015, pp. 78–83, doi: 10.1109/GCCT.2015.7342627.
- [26] Z. Xie and Q. Wang, "Large space fire detection in laboratory-scale based on color image segmentation," in *Proceedings - 9th International Symposium on Distributed Computing and Applications to Business, Engineering and Science, DCABES 2010*, Aug. 2010, pp. 572–575, doi: 10.1109/DCABES.2010.122.

BIOGRAPHIES OF AUTHORS






Nguyen Hung Khanh    received his B.S. in Mechatronics Engineering from Lachong University, Vietnam, in 2008, MS in Precision Mold and Die from National Kaohsiung University of Applied Sciences, Kaohsiung City, Taiwan, in 2011. Currently, he is a member of Dong Nai Technology University, Bien Hoa City, Vietnam. His research interests focus on heat transfer engineering, mechanical engineering, and electrical and electronic engineering. He can be contacted at email: nguyenhungkhanh@dnut.edu.vn.






Nguyen Le Thai    received his B.S. in Electronic engineering from Danang University of Science and Technology, Vietnam, in 2003, MS in Electronic Engineering from Posts and Telecommunications Institute of Technology, Ho Chi Minh, Vietnam, in 2011 and Ph.D. degree of Mechatronics Engineering from Kunming University of Science and Technology, China, in 2016. He is currently with the Nguyen Tat Thanh University, Ho Chi Minh City, Vietnam. His research interests include the renewable energy, optimisation techniques, robust adaptive control, and signal processing. He can be contacted at email: nlthai@ntt.edu.vn.






Thuc Minh Bui    got his B.S. and M.S. degrees in Electrical Engineering from Ho Chi Minh City University of Technology and Education in 2005 and 2008, respectively, and his Ph.D. degree in Electrical Engineering at from Yeungnam University in Gyeongsan, Korea, in 2018. He is currently a lecturer at the Faculty of Electrical and Electronics Engineering at Nha Trang University in Nha Trang City, Vietnam. His scientific interests include control theory, power converter, automation, and optical science with applications to industry and the environment. He can be contacted at email: minhbt@ntu.edu.vn.



Huu Phuc Dang    received a Physics Ph.D. degree from the University of Science, Ho Chi Minh City, in 2018. Currently, he is a lecturer at the Faculty of Fundamental Science, Industrial University of Ho Chi Minh City, Ho Chi Minh City, Vietnam. His research interests include simulation LEDs material, and renewable energy. He can be contacted at email: danghuophuc@iuh.edu.vn.



Huynh Thanh Thien    received the Ph.D. degree in Electrical and Computer Engineering from the University of Ulsan, Ulsan, South Korea. He is working as a lecturer at the Faculty of Electrical and Electronics Engineering, Ton Duc Thang University, Ho Chi Minh City, Vietnam. His research interests include cognitive radio and next-generation wireless communications systems, game theory, deep learning, reinforcement learning, and semiconductor device. He can be contacted at email: huynhthanhthien@tdtu.edu.vn.